PHYSICAL REVIEW A **93**, 041803(R) (2016)

Localized $\mathcal{PT}$-symmetric directionally invisible scatterers

Elisa Hurwitz and Greg Gbur*
Department of Physics and Optical Science, University of North Carolina, Charlotte, North Carolina 28223, USA
(Received 29 January 2016; published 21 April 2016)

We demonstrate how to create localized $\mathcal{PT}$-symmetric directionally invisible scatterers directly from a governing wave equation. Moreover, we can construct general non-$\mathcal{PT}$-symmetric objects which exhibit directional invisibility, though such an effect is typically associated with $\mathcal{PT}$-symmetric objects. Whereas previously the determining condition for an optical $\mathcal{PT}$-symmetric device was a $\mathcal{PT}$-symmetric complex refractive index, we show that a broader condition, requiring only the scattering potential to be $\mathcal{PT}$-symmetric, leads to the same behavior. This enables the construction of $\mathcal{PT}$-symmetric objects without a $\mathcal{PT}$-symmetric complex refractive index, effectively doubling the number of possible invisible objects. Consequently, the set of gain-loss invisible objects is much broader than previously realized, and several examples are shown.

DOI: 10.1103/PhysRevA.93.041803

In the study of Schrödinger's equation, it was long assumed that Hermitian Hamiltonians are required to guarantee that a system's energy eigenvalues are real [1,2]. The discovery that a wide class of non-Hermitian Hamiltonians can still show entirely real spectra, if they are parity-time ($\mathcal{PT}$)-symmetric [3], therefore has attracted much attention. In optics, it has been suggested that the complex refractive index $n(\mathbf{r}) = n_R(\mathbf{r}) + in_I(\mathbf{r})$ is analogous to the quantum mechanical potential, where the real part of the refractive index must be a symmetric function of position $\mathbf{r}$, i.e., $n_R(\mathbf{r}) = n_R(-\mathbf{r})$, while the imaginary part of $n(\mathbf{r})$ must be an antisymmetric function of $\mathbf{r}$, i.e., $n_I(\mathbf{r}) = -n_I(-\mathbf{r})$, to achieve $\mathcal{PT}$-symmetric behavior [4,5]. A number of these $\mathcal{PT}$-symmetric systems have exhibited directional invisibility—they are perfectly reflectionless for one direction of illumination and strongly scattering in the opposite direction [6,7]—suggesting a close relationship between invisibility and $\mathcal{PT}$ symmetry.

These systems have, however, almost entirely been investigated in layered, gain-loss, infinite slab geometries [8,9], with the exception of two studies: One considers a specific localized $\mathcal{PT}$-symmetric scatterer designed using transformation optics [10], while the other explores a $\mathcal{PT}$-symmetric cylindrical cloak with a gain coating on the incident side and a loss coating on the exiting side for a microwave plane wave [11].

Recently, Gbur introduced a new technique [12] to design a wide variety of directionally invisible objects directly and without approximation from the governing wave equation, subject to a number of boundary conditions. The problem is framed in terms of classical scattering theory, in which the object or scatterer is described by a scattering potential instead of by its refractive index. Within this framework, the analogy between the time-independent Schrödinger equation, in terms of the quantum mechanical potential, and the Helmholtz equation, in terms of the scattering potential, evinces the relationship between $\mathcal{PT}$ symmetry in quantum mechanics and $\mathcal{PT}$ symmetry in optics.

In this Rapid Communication, we explore the role $\mathcal{PT}$ symmetry plays in achieving directionally invisible scatterers, using the newly developed technique for constructing such objects. It is shown that $\mathcal{PT}$ symmetry is not a necessary condition for the scatterer to be directionally invisible. It is possible to design both $\mathcal{PT}$-symmetric and non-$\mathcal{PT}$-symmetric directionally invisible objects, and an example of each is presented. It is also shown that requiring the complex scattering potential, instead of the complex refractive index, to be $\mathcal{PT}$-symmetric reveals a larger set of invisible structures. Consequently, if the scattering potential is $\mathcal{PT}$-symmetric, there are two distinct solutions for the complex refractive index. This implies that for an invisible object with a $\mathcal{PT}$-symmetric refractive index, there is an object that is also invisible with a complementary anti-$\mathcal{PT}$-symmetric refractive index.

We begin by considering an object of refractive index $n(\mathbf{r})$, illuminated by a scalar monochromatic plane wave $U^{(i)}(\mathbf{r})$. The total field $U(\mathbf{r})$ satisfies the Helmholtz equation with an inhomogeneous wave number,

$$[\nabla^2 + n^2(\mathbf{r})k^2]U(\mathbf{r}) = 0, \tag{1}$$

where $k = \frac{\omega}{c} = \frac{2\pi}{\lambda}$, ω is the frequency, λ is the wavelength, and c is the vacuum speed of light. Introducing the scattering potential $F(\mathbf{r})$ of the form

$$F(\mathbf{r}) = \frac{k^2}{4\pi}[n^2(\mathbf{r}) - 1] \tag{2}$$

and writing $U(\mathbf{r}) = U^{(i)}(\mathbf{r}) + U^{(s)}(\mathbf{r})$, where $U^{(i)}(\mathbf{r}) = U_0 e^{ik\hat{\mathbf{s}}_0\cdot\mathbf{r}}$ and $U^{(s)}(\mathbf{r})$ are the incident and scattered fields, respectively, it is possible to write an inhomogeneous wave equation for the scattered field [13],

$$(\nabla^2 + k^2)U^{(s)}(\mathbf{r}) = -4\pi F(\mathbf{r})U(\mathbf{r}). \tag{3}$$

Because the scattered field is present on both sides of Eq. (3), it is generally not possible to solve this equation analytically. However, we may find a nonscattering solution by the following procedure. First, we define

$$U^{(s)}(\mathbf{r}) = U^{(i)}(\mathbf{r})U^{(\mathrm{loc})}(\mathbf{r}), \tag{4}$$

where $U^{(\mathrm{loc})}(\mathbf{r})$ is termed the *local scattered field* of the inhomogeneous scatterer; it is the scattered field with the oscillations of the incident field removed [12]. Next, we apply techniques originally introduced to design *nonradiating sources* [14] to design invisible objects. In this case, the

*gjgbur@uncc.edu

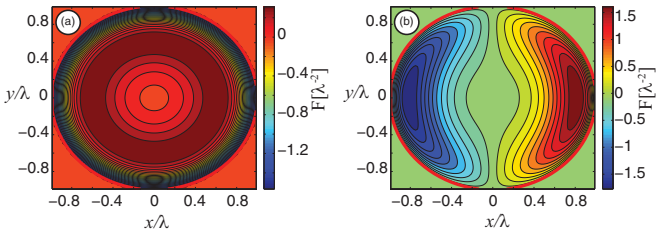

FIG. 1. Real part (a) and imaginary part (b) of the scattering potential $F(\mathbf{r})$ associated with Eq. (7), ($a = 1$).

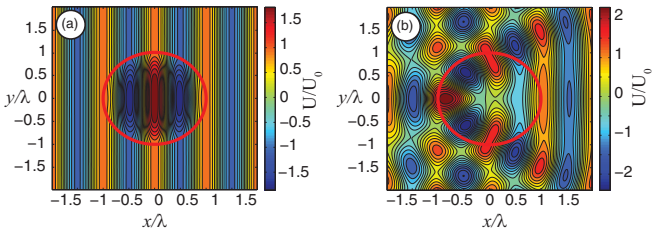

FIG. 2. Real part of the total field (incident + scattered) when the incident plane wave ($\lambda = 1$) propagates in (a) the positive $\hat{\mathbf{x}}$ direction ($\theta = 0^\circ$) and (b) the negative $\hat{\mathbf{x}}$ direction ($\theta = 180^\circ$). The circles indicate the domain of the scatterer, which has a radius $a = 1$. U_0 is the incident field amplitude.

same boundary conditions which are typically applied to nonradiating sources [15] are applied to the local field $U^{(\mathrm{loc})}(\mathbf{r})$ that defines the invisible object, namely,

$$U^{(\mathrm{loc})}(\mathbf{r})\big|_S = 0, \text{ and } \frac{\partial}{\partial n}U^{(\mathrm{loc})}(\mathbf{r})\bigg|_S = 0, \tag{5}$$

where $\frac{\partial}{\partial n}$ represents the derivative normal to the surface S, which forms the boundary of the scatterer. The scattered field $U^{(\mathrm{loc})}(\mathbf{r}) = 0$ outside of the scatterer. Writing the total field as $U(\mathbf{r}) = [1 + U^{(\mathrm{loc})}(\mathbf{r})]U^{(i)}(\mathbf{r})$ and substituting it with Eq. (4) into Eq. (3), one can directly solve for the scattering potential $F(\mathbf{r})$ that produces the scattered field, i.e.,

$$F(\mathbf{r}) = -\frac{1}{4\pi}\frac{\nabla^2 U^{(\mathrm{loc})}(\mathbf{r}) + 2ik\hat{\mathbf{s}}_0 \cdot \nabla U^{(\mathrm{loc})}(\mathbf{r})}{1 + U^{(\mathrm{loc})}(\mathbf{r})}. \tag{6}$$

We now note that a remarkable effect of this construction is that any real-valued, mirror symmetric $U^{(\mathrm{loc})}(\mathbf{r})$ will result in a localized, $\mathcal{PT}$-symmetric directionally invisible object. This occurs because the numerator of Eq. (6) consists of a real, symmetric operation on $U^{(\mathrm{loc})}(\mathbf{r})$ and an imaginary, antisymmetric operation on $U^{(\mathrm{loc})}(\mathbf{r})$, while the denominator is real and symmetric.

To demonstrate such a $\mathcal{PT}$-symmetric invisible object, we consider a two-dimensional scatterer with $\hat{\mathbf{s}}_0 = \hat{\mathbf{x}}$ and $U^{(\mathrm{loc})}(\mathbf{r})$ given by

$$U^{(\mathrm{loc})}(\mathbf{r}) = \cos^2\left(\frac{\pi r^2}{2a^2}\right), \quad |r| \leqslant a, \tag{7}$$

where $r = \sqrt{x^2 + y^2}$ and a is the radius of the scatterer. The potential is found by substituting Eq. (7) into Eq. (6). The fields inside and outside of the scatterer are then calculated using a Green's function method similar to that used in electromagnetic scattering theory [16]. The calculated real and imaginary parts of the scattering potential can be seen to be symmetric and antisymmetric, respectively, with respect to position along the $\hat{\mathbf{x}}$ axis, as shown in Fig. 1. When a plane wave ($\lambda = 1$) is incident from the left (the invisibility direction), there is no scattered field [Fig. 2(a)], whereas there is strong scattering when a plane wave is incident from the opposite direction [Fig. 2(b)]. Unidirectional perfect transmission has been observed in other $\mathcal{PT}$-symmetric structures, for example, in optically coupled fibers [6] and a unidirectional reflectionless fiber [7]. The lack of reflection for one direction in those cases was demonstrated by calculating and measuring the transmission and reflection coefficients for both directions. Perfect transmission is achieved by balancing gain and loss for one direction of propagation. To compare these results to our two-dimensional scatterers, we use the scattering and extinction cross sections. In the two-dimensional case, the extinction cross section is the ratio of the rate of change at which the energy is removed from the incident wave normalized by the flux of incident energy; the result is a quantity with units of length. The scattering cross section is the ratio of the total power scattered by the object normalized by the flux of incident energy, also with units of length.

Some time ago, Alexopoulos and Uzunoglu [17] showed that while passive spherical particles (with loss only) always possess a nonzero scattering and extinction cross section, an active particle (with gain only) can have zero extinction cross section. Not long after, however, Kerker showed that true invisibility requires that both the scattering and the extinction cross sections be equal to zero [18]; this is the criterion we adopt in this paper. The equations leading to the expressions for the extinction and scattering cross sections for two-dimensional scatterers are outlined here. The scattering amplitude $f(\hat{\mathbf{s}},\hat{\mathbf{s}}_0)$ is calculated from the following relationship for large r:

$$U^{(s)}(r\hat{\mathbf{s}}) = f(\hat{\mathbf{s}},\hat{\mathbf{s}}_0) i\pi H_0^{(1)}(kr), \tag{8}$$

where $H_0^{(1)}(kr)$ is the zeroth-order Hankel function of the first kind. This shows the dependence of the scattered field on the scattering amplitude and the scattering potential. The extinction cross section of the scattering object [13] is given in terms of the forward-scattering amplitude $f(\hat{\mathbf{s}}_0,\hat{\mathbf{s}}_0)$ by

$$Q^{(\mathrm{ext})} = Q^{(\mathrm{abs})} + Q^{(\mathrm{sca})} = \frac{4\pi}{k}\mathrm{Im}\{f(\hat{\mathbf{s}}_0,\hat{\mathbf{s}}_0)\}, \tag{9}$$

where $Q^{(\mathrm{ext})}$ is the extinction cross section, $Q^{(\mathrm{abs})}$ is the absorption cross section, and $Q^{(\mathrm{sca})}$ is the scattering cross section. Since both the incident and scattering directions are $\hat{\mathbf{s}}_0$, and $\hat{\mathbf{s}}_0$ is the forward direction, $f(\hat{\mathbf{s}}_0,\hat{\mathbf{s}}_0)$ is also called the forward-scattering amplitude. The scattering cross section $Q^{(\mathrm{sca})}$ may be written in terms of the scattering amplitude as follows:

$$Q^{(\mathrm{sca})} = \int_L |f(\hat{\mathbf{s}},\hat{\mathbf{s}}_0)|^2\, dl, \tag{10}$$

where L is the boundary outside of the scatterer. The scattering cross section is calculated by combining Eqs. (10) and (8).

We calculated the extinction and scattering cross sections for all directions of incidence $\hat{\mathbf{s}}_0$. Dividing the extinction and scattering cross sections by the geometric cross section of

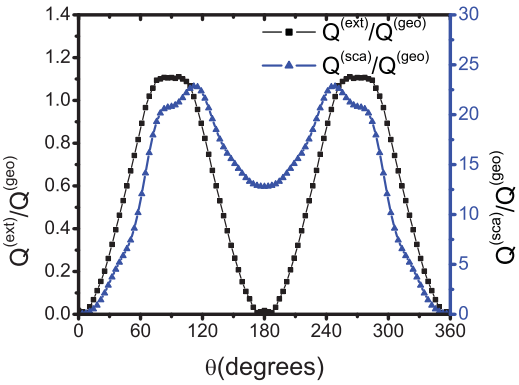

FIG. 3. Extinction and scattering cross sections as a function of incident angle [$\mathcal{PT}$-symmetric example, Eq. (7)].

the scatterer, $Q^{(\mathrm{geo})} = 2\lambda$, connects the cross section of the energy extinguished or scattered to the size of the object. In the invisibility direction ($\theta = 0^\circ$), both $Q^{(\mathrm{ext})}$ and $Q^{(\mathrm{sca})}$ are equal to zero (Fig. 3). In the opposite direction ($\theta = 180^\circ$), there is strong scattering, and, consequently, $Q^{(\mathrm{sca})} \neq 0$. Nevertheless, for the opposite direction $Q^{(\mathrm{ext})} = 0$: due to the presence of the gain medium, it is possible to have strong scattering and no extinction of the illuminating wave. This phenomenon is analogous to that observed in Ref. [8] for a $\mathcal{PT}$-symmetric layered scatterer. Taking a closer look at Fig. 2(b) reveals that when the wave is incident at $\theta = 180^\circ$, the wave preferentially scatters in specific directions. It may be of note that these preferred scattering directions coincide with the peaks of the scattering cross section (Fig. 3).

A question of some interest is the robustness of the invisibility when the object is not perfect, for example, when errors in manufacturing occur. There are many ways to simulate such imperfections, such as adding spherical harmonic terms or periodic linear distributions to the scattering potential. To estimate the effect of manufacturing error, a periodic error of the form $c \times (\%\ \text{error}) \times \max|F(\mathbf{r})| \cos 2\pi f x$ was added to the scattering potential $F(\mathbf{r})$ and a Monte Carlo simulation was performed for the invisibility direction of the scatterer. The spatial frequency was arbitrarily set to $f = 6k$. The amplitude c representing the percent error was chosen from a Gaussian distribution of values between 0 and 1. The $\max|F(\mathbf{r})|$ value is the maximum value of the absolute value of the $F(\mathbf{r})$ over its entire domain without any error introduced. The simulation was run 10 times for each percentage of error ranging from zero to 10% in increments of 1%. At 10% error $Q^{(\mathrm{ext})}/Q^{(\mathrm{geo})} = 0.03679 \pm 0.02911$ and $Q^{(\mathrm{sca})}/Q^{(\mathrm{geo})} = 0.07734 \pm 0.03388$. These numbers are only slightly larger than the values for the perfect scatterer, $Q^{(\mathrm{ext})}/Q^{(\mathrm{geo})} = 0.01775$ and $Q^{(\mathrm{sca})}/Q^{(\mathrm{geo})} = 0.02431$, which are only due to computational effects.

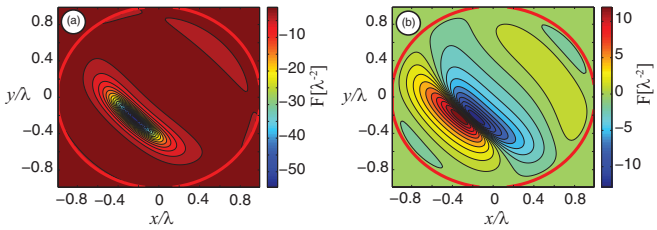

FIG. 4. Real (a) and imaginary (b) parts of the scattering potential for a non-$\mathcal{PT}$-symmetric nonscattering scatterer ($a = 1$).

We may also use the method to design invisible objects that are gain-loss but not $\mathcal{PT}$-symmetric. It turns out that they share many properties with their $\mathcal{PT}$-symmetric counterparts. A simple local function that results in a non-$\mathcal{PT}$-symmetric scattering potential is given by

$$U^{(\mathrm{loc})}(\mathbf{r}) = \sin\pi(x+y)\cos^2\left(\frac{\pi r^2}{2a^2}\right), \quad |r| \leqslant a. \tag{11}$$

The real and imaginary parts of the scattering potential associated with the $U^{(\mathrm{loc})}(\mathbf{r})$ in Eq. (11) are shown in Fig. 4. Neither one has any particular spatial symmetry. When the wave is incident on the scatterer in the invisibility direction ($+\hat{\mathbf{x}}$ direction) the scattered field is localized to the domain of the scatterer, and the object is invisible outside of its domain [Fig. 5(a)]. In contrast, when the wave is incident on the scatterer in the opposite direction, the object produces a strong scattered field [Fig. 5(b)]. Again, in the invisibility direction both the extinction and the scattering cross sections are equal to zero, but in the opposite direction only the extinction cross section is equal to zero [Fig. 5(c)]. Here, again the preferred scattering directions appear to coincide with the peak of the scattering cross sections [Fig. 5(b) and 5(c)]. In contrast to the $\mathcal{PT}$-symmetric case, where both the scattering and extinction cross sections are symmetric [Fig. 3(c)], in this case

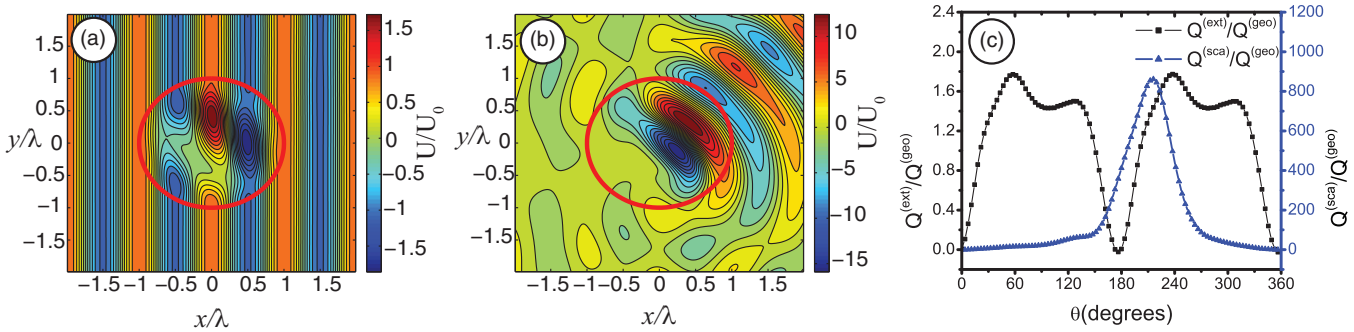

FIG. 5. Real part of the total field (incident + scattered) when the incident plane wave propagates in (a) the positive $\hat{\mathbf{x}}$ direction ($\theta = 0^\circ$) and (b) the negative $\hat{\mathbf{x}}$ direction ($\theta = 180^\circ$). The fields are scaled to the incident field amplitude U_0. The circles indicate the domain of the scatterer, which has a radius of $a = 1$. The extinction and scattering cross sections are shown in (c) for all angles θ or incidence.

the extinction and scattering cross sections are asymmetric [Fig. 5(c)].

In our examples, $F(\mathbf{r})$ determines whether or not the object is $\mathcal{PT}$-symmetric, not $n(\mathbf{r})$; this means that there are two values of $n(\mathbf{r})$ for each $F(\mathbf{r})$. To explore the role of the symmetries of each component, we substitute the complex definitions of refractive index $n(\mathbf{r}) = n_R(\mathbf{r}) + in_I(\mathbf{r})$ and the scattering potential $F(\mathbf{r}) = F_R(\mathbf{r}) + iF_I(\mathbf{r})$ into Eq. (2), and obtain for the real and imaginary parts of the scattering potential

$$F_R(\mathbf{r}) = \frac{k^2}{4\pi}\left[n_R^2(\mathbf{r}) - n_I^2(\mathbf{r}) - 1\right], \tag{12a}$$

$$F_I(\mathbf{r}) = \frac{k^2}{4\pi} 2n_I(\mathbf{r})n_R(\mathbf{r}). \tag{12b}$$

If $\mathcal{PT}$ symmetry is defined by a symmetric real $F_R(\mathbf{r})$ and an antisymmetric $F_I(\mathbf{r})$ with respect to the position $\mathbf{r}$, then the simplest $\mathcal{PT}$-symmetric potentials will have either n_R or n_I symmetric, and n_I or n_R antisymmetric with respect to position, respectively. Therefore, requiring that the refractive index be $\mathcal{PT}$-symmetric forces the scattering potential to be $\mathcal{PT}$-symmetric but the converse does not hold true. Therefore, requiring the refractive index to be $\mathcal{PT}$-symmetric only results in half of the $\mathcal{PT}$-symmetric solutions for the scattering potential. This relationship between the scattering potential $F(\mathbf{r})$ and the refractive index $n(\mathbf{r})$ is also true for the non-$\mathcal{PT}$-symmetric objects.

The construction technique introduced here can be readily extended to electromagnetic waves, and it seems likely that it can be extended to scatterers which are invisible for multiple directions of illumination. It is also possible to apply this technique with different types of incident waves, for example, one focused through a point, by rederiving an expression for scattering potential with a different $U^{(i)}(\mathbf{r})$, provided that there are no zeros in $U^{(i)}(\mathbf{r})$. Also, as shown in [8], it is possible to extend the technique to make $\mathcal{PT}$-symmetric directional cloaks by requiring that $U^{(\mathrm{loc})}(\mathbf{r}) = -U^{(i)}(\mathbf{r})$ at the inner boundary of the cloak and applying the boundary conditions in Eq. (5) at the outer boundary of the cloak. An arbitrary object may then be hidden inside the cloak for the directions determined by the scattering potential.

Because the time-independent Schrödinger equation is analogous to the Helmholtz equation, the method presented here to design directionally invisible scatterers by applying specific conditions to the scattering potential can be readily applied to quantum mechanical systems by applying similar specific conditions to the quantum mechanical potential.

In summary, a method to construct both $\mathcal{PT}$-symmetric and non-$\mathcal{PT}$-symmetric directionally invisible scatterers has been demonstrated. It requires that the scattering potential be $\mathcal{PT}$-symmetric instead of the refractive index, increasing the number of possible $\mathcal{PT}$-symmetric solutions and relaxing the $\mathcal{PT}$-symmetry conditions imposed on the refractive index.

Furthermore, because the function $U^{(\mathrm{loc})}(\mathbf{r})$ is only constrained to be smooth and to satisfy Eq. (5), it is possible to create invisible gain-loss structures that have no particular symmetry. The technique and observations presented here demonstrate that a much broader variety of effectively $\mathcal{PT}$-symmetric objects exist in optics. In addition, they suggest a stronger connection between invisibility and $\mathcal{PT}$ symmetry than previously appreciated. Therefore, the set of gain-loss invisible objects is much larger than previously realized, and we have demonstrated a technique that, in principle, allows construction of all gain-loss directionally invisible objects.

The authors thank Dr. Angela Davies from the Department of Physics and Optical Science at UNC Charlotte for helpful suggestions on how to simulate manufacturing error.

[1] C. M. Bender, Contemp. Phys. **46**, 277 (2005).
[2] C. M. Bender, J. Phys.: Conf. Ser. **631**, 012002 (2015).
[3] C. M. Bender and S. Boettcher, Phys. Rev. Lett. **80**, 5243 (1998).
[4] R. El-Ganainy, K. G. Makris, D. N. Christodoulides, and Z. H. Musslimani, Opt. Lett. **32**, 2632 (2007).
[5] K. G. Makris, R. El-Ganainy, D. N. Christodoulides, and Z. H. Musslimani, Phys. Rev. Lett. **100**, 103904 (2008).
[6] C. Rüter, K. Makris, R. El-Ganainy, D. Christodoulides, M. Segev, and D. Kip, Nat. Phys. **6**, 192 (2010).
[7] Z. Lin, H. Ramezani, T. Eichelkraut, T. Kottos, H. Cao, and D. N. Christodoulides, Phys. Rev. Lett. **106**, 213901 (2011).
[8] L. Feng, Y.-L. Xu, W. Fegadolli, M.-H. Lu, J. Oliveira, V. Almeida, Y.-F. Chen, and A. Scherer, Nat. Mater. **12**, 108 (2013).
[9] A. Regensburger, C. Bersch, M.-A. Miri, G. Onishchukov, D. N. Christodoulides, and U. Peschel, Nature **488**, 167 (2012).
[10] X. Zhu, L. Feng, P. Zhang, X. Yin, and X. Zhang, Opt. Lett. **38**, 2821 (2013).
[11] D. L. Sounas, R. Fleury, and A. Alù, Phys. Rev. Appl. **4**, 014005 (2015).
[12] G. Gbur, Opt. Lett. **40**, 986 (2015).
[13] M. Born and E. Wolf, *Principles of Optics*, 7th ed. (Cambridge University Press, Cambridge, England, 1999), Chap. 13.
[14] G. Gbur, in *Progress in Optics*, Vol. 45, edited by E. Wolf (Elsevier, New York, 2003), pp. 273–315.
[15] A. Gamliel, K. Kim, A. I. Nachman, and E. Wolf, J. Opt. Soc. Am. A **6**, 1388 (1989).
[16] O. J. F. Martin and N. B. Piller, Phys. Rev. E **58**, 3909 (1998).
[17] N. G. Alexopoulos and N. K. Uzunoglu, Appl. Opt. **17**, 235 (1978).
[18] M. Kerker, Appl. Opt. **17**, 3337 (1978).